JOURNAL OF AIRCRAFT
Vol. 43, No. 2, March–April 2006

Near-Field Wing-Tip Vortices and Exponential Vortex Solution

H. J. Zhang*
China Institute of Metrology, 310018 Hangzhou, People's Republic of China
Y. Zhou†
Hong Kong Polytechnic University, Hung Hom, Kowloon, Hong Kong, People's Republic of China
and
J. H. Whitelaw‡
Imperial College London, London, England SW7 2BX, United Kingdom

Vortices shed from the tip of a rectangular half-span wing model (NACA 0012) have been investigated with particle image velocimetry at a chord Reynolds number between 3.4×10^4 and 26.6×10^4 and angles of attack $\alpha = 8$ and 16 deg over $0.2 \sim 5$ chord lengths downstream of the model. It has been found that the measured wing-tip vortex shows little dependence in the circumferential velocity v_θ and vorticity Ω, when normalized by their local maximum, on α, Reynolds number, and downstream distance from the wing. Furthermore, the radial distributions of v_θ and Ω coincide quite well with the exponential vortex solution, with only a slight departure outside the core region.

Nomenclature

c	=	chord length of the wing
N	=	number of the captured particle image velocimetry images
Re	=	Reynolds number ($\equiv U_\infty c/\nu$)
r	=	radius from the tip vortex center
r_c	=	core radius of the tip vortex
U_∞	=	freestream velocity
v_r	=	radial velocity
v_θ	=	circumferential velocity
$v_{\theta,\max}$	=	maximum circumferential velocity
x, y, z	=	coordinates in the streamwise, lateral, and spanwise directions, respectively
α	=	angle of attack
Γ	=	vortex circulation
Γ_c	=	circulation within the vortex core
Γ_0	=	initial circulation of the exponential vortex solution
θ	=	azimuthal location
ν	=	kinematic viscosity of the air
ω	=	vorticity
$\omega_{\max}$	=	maximum vorticity at the vortex center
ω_0	=	initial vorticity of the exponential vortex solution

Introduction

TIP vortices are present in the wake of lifting wings and are responsible for many adverse phenomena, such as the hazard of a large aircraft posed to the following smaller aircraft and the noise created by vortex interactions between neighboring blades of a helicopter rotor. They have been the subject of extensive research for many decades[1–7] but less so in the past decade for reasons such as the perceived lack of urgency. It is clear, however, that airport capacity will be insufficient in the coming years, as witnessed by discussions of new runways in Hong Kong and in the south east of England, so that new attempts to understand and control tip vortices are required.

Vortices are generated from the tip of lifting wings and roll up as they are transported downstream. Their downstream evolution may be divided into three stages, that is, rollup (<20 spans), vortex region (200 spans), and decay (>500 spans).[8] The near-field behavior of the vortices is important because manipulation has to begin with the wing or wait for the Crow[9] instability, which generally requires very large distances to have an effect. Some studies of the near field of wing-tip vortices are described in Refs. 10–14. Chow et al.,[10] for example, examined the rollup process of wing-tip vortices in the very near wake, up to $x/c = 0.678$ (where x is the downstream distance from the trailing edge), in terms of the mean flowfield and Reynolds stress tensor. They found that the axial velocity in the vortex core reached 1.77 times the freestream velocity just upstream of the trailing edge and turbulence levels in and around the vortex were initially very large but decayed rapidly. Shekarriz et al.[11] found that the rollup of the tip vortex was completed almost immediately downstream of the trailing edge of the wing ($x/c < 1$) and that the overall circulation of this vortex remained nearly constant throughout the range $0 < x/c < 6.7$. Smith[14] measured with a particle image velocimeter and found rapid formation of the tip vortex with 50% of circulation in the wake residing within the vortex core at the trailing edge. However, the subsequent rollup of the trailing-edge shear layer occurred at a much slower rate, and the wake could not be regarded as fully rolled up even at $10c$ downstream of the wing.

Flow velocity has usually been measured by pressure probe, hot-wire probe, and laser-Doppler anemometry, which may enable three-dimensional aspects and statistical information to be examined at sequential single locations. Particle-image velocimetry (PIV) provides an alternative in which the flowfield can be visualized and quantified in terms of instantaneous images of the velocity field with sequential images separated by less than a second so that averages can be assembled in relatively short periods. Bearman and Hogan[15] used PIV in a laboratory wind tunnel to capture the streamwise vortical structure behind a delta wing, and Huenecke and Huenecke[16] used it in a large-scale production wind tunnel with considerable success. Nevertheless, there has been limited application to the study of the details of vortices,[17] which provides a motivation for the present study.

The exponential vortex solution or Lamb–Oseen vortex has been used to model vortical structures in a turbulent flow (see Ref. 18), for example, by Davies[19] in the planar near wake of a D-shape cylinder, by Oler and Goldschmidt[20] in the self-preserving region of a plane jet, and by Bisset et al.[21] in the self-preserving far wake of a circular cylinder. The direct numerical simulations of a turbulent boundary

Received 4 February 2005; revision received 13 May 2005; accepted for publication 16 May 2005.

*Associate Professor, Department of Metrological Technology and Engineering.
†Associate Professor, Department of Mechanical Engineering.
‡Professor, Department of Mechanical Engineering.

layer of Robinson[22] showed that quasi-streamwise vortices near the wall resemble Lamb–Oseen vortices. It would be interesting to see whether the exponential vortex solution could be used to model the wing-tip vortex.

The paper is organized as follows. The measurement technique and experimental details are given in the following section. In the "Results and Discussions," section, the measurement results of the near-field wing-tip vortices and a comparison between the exponential vortex solution and the measured wing-tip vortices are presented. The work is concluded in Conclusions.

Experimental Details

Experiments were carried out in a closed-loop low-speed wind tunnel with a square working section (0.6×0.6 m) and length of 2.4 m (Ref. 23). The freestream velocity in the working section is up to 50 m/s. A half-span, rectangular plane airfoil (NACA 0012) with a chord of 0.25 m and a span of 0.4 m was mounted horizontally in the test section with its leading edge 0.2 m downstream from the tunnel contraction (Fig. 1). Measurements were performed at $U_\infty = 2.0 \sim 15.6$ m/s ($Re = 3.4 \sim 26.6 \times 10^4$) and $\alpha = 8$ and 16 deg, respectively. In this wind-speed range, the turbulence intensity is less than 0.2% in the working section.

The PIV measurements made use of a commercial system (Dantec 2100) and a smoke generator (Teknova, Model RG 100) with paraffin oil to produce droplets of around 1 μm in diameter. The flow was illuminated in a plane (about 3 mm in thickness) perpendicular to the main flowstream by double-pulsed YAG laser (NewWave) at a wavelength of 532 nm, with a maximum energy output of 120 mJ. A plane mirror (height times width $= 0.3 \times 0.15$ m) was placed downstream of the light sheet plane at a distance of about $2c$ from the laser sheet so that the image on the light sheet could be projected out of the test section and captured by a charge-coupled device camera (HiSense Type 13, 1280×1024 pixels). Note that the mirror will produce, as a large blunt object, eddies that may influence not only the downstream flow but also the upstream, including the wing-tip vortex behaviors. This effect was assessed by examining the PIV data obtained at various distances between the laser sheet and the mirror. It has been found that, once the distance exceeded $2c$, the influence was less than 5% on the scattering of vortex centers and less than 2% on the maximum vortcity. We have also conducted a test by putting the camera (which is considerably smaller in size than the mirror), instead of the mirror, into the wind tunnel when capturing the PIV images, but found no difference in the experimental results. It may be concluded that the unsteadiness due to the mirror is negligibly small.

A Dantec FlowMap Processor synchronized image taking and illumination. Each image covered a view area typically of 135×106 mm. The image processing involved rectangular interrogation areas, each including 32 pixels with a 25% overlap area in both the horizontal and vertical directions. The horizontal and vertical image magnifications were identical, at 0.1 mm/pixel and a typical spatial resolution for vorticity estimate was about 2.60 mm or $0.01c$. Each laser pulse lasted for 0.01 μs, and the interval between successive pulses varied from 100 to 20 μs for freestream velocities from 2.0 to 15.6 m/s. Thus, a particle would travel 0.2–0.3 mm (2–3 pixels) between exposures. Because the span of the wing is 0.4 m, $1.6c$, the measured tip vortex radius is in the order of 0.1–$0.2c$, much smaller than $1.6c$. Furthermore, the boundary layer of the wall is in the order of 10 mm or $0.04c$, very thin compared with the span. It is believed that the wall effect on the wake concerned is negligibly small. Therefore, no correction was made on the measured data.

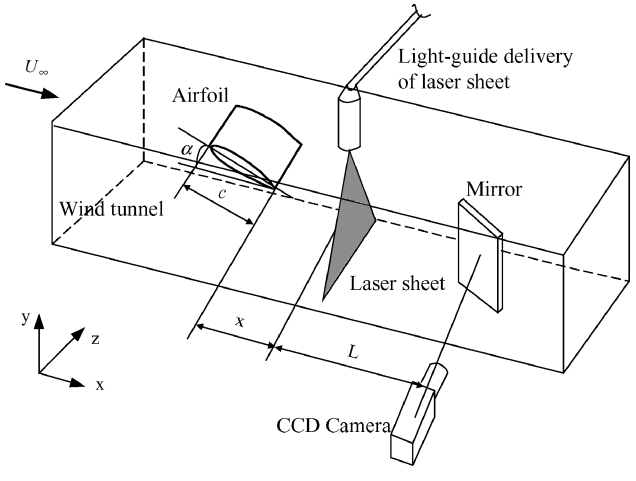

Fig. 1 Schematic of experimental setup.

Results and Discussion

Characteristics of the Tip Vortex

Preliminary tests indicated that leading-edge flow separation from the airfoil began with α of about 14 deg at the present Reynolds numbers, and it is known from Huang and Lin[24] that separation from the same type of airfoil began at 12 deg with a Reynolds number of about 8×10^4. The data presented focus on $\alpha = 8$ and 16 deg, which represent the cases with and without leading-edge separation, respectively. Figure 2 shows typical photographs of the tip vortex visualized at $x/c = 3$. At both α values, some smaller-scale secondary structures are discernable, as previously observed by Francis and Katz[13] and Yeung and Lee.[17] Note that the two images were obtained in the same plane using an identical camera setup. Apparently, the tip vortex at $\alpha = 16$ deg is markedly larger.

The tip vortex varies in shape, center position, and strength from one image to another and cannot be well characterized by one image. Thus, the averaged circumferential velocity and vorticity distributions with respect to the tip vortex center were calculated based on 100 images. For instance, the circumferential velocity was

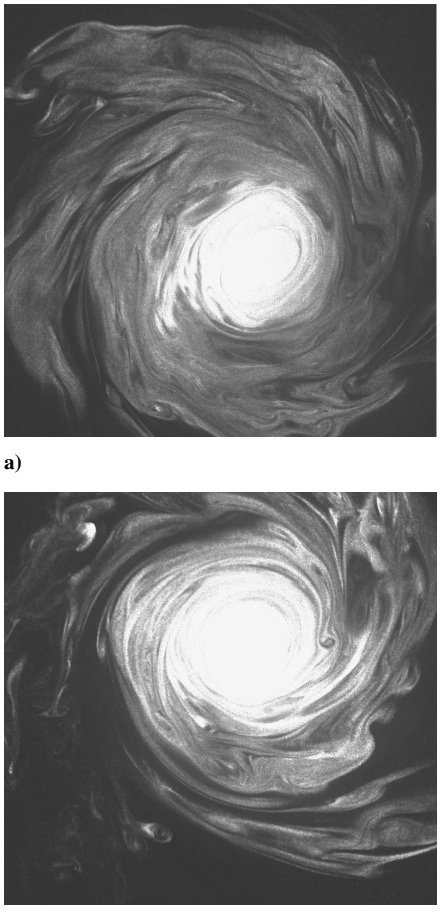

a)

b)

Fig. 2 Flow visualization images of tip vortices at $x/c = 3$ and $Re = 7.6 \times 10^4$: a) $\alpha = 8$ deg and b) $\alpha = 16$ deg.

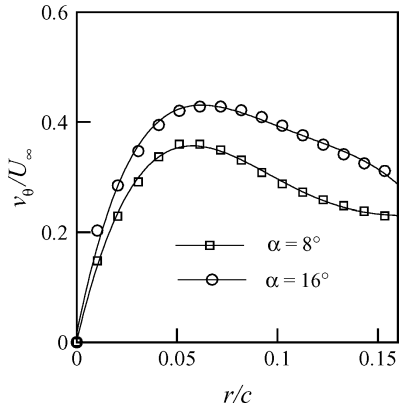

Fig. 3 Averaged circumferential velocity of tip vortices, v_θ/U_∞, at $x/c = 3$ and $Re = 7.6 \times 10^4$.

calculated as

$$v_\theta(r) = \frac{1}{100k}\sum_{1}^{100}\sum_{i=1}^{k} v_{\theta,i}(y,z)|_{y^2+z^2=r^2}$$

where k is the number of points for each radius, $r = \sqrt{(y^2+z^2)}$. Figure 3 shows the circumferential velocity distributions at $x/c = 3$. Define the core radius r_c of the tip vortex as that where the maximum circumferential velocity $v_{\theta,\max}$ occurs. The normalized value r_c/c is about 0.05 for $\alpha = 8$ deg and 0.06 for $\alpha = 16$ deg. The tip vortex core grew with α, though not by a great deal, which is in agreement with the flow visualizations (Fig. 2). On the other hand, $v_{\theta,\max}/U_\infty$ increases from about 0.37 to 0.44 as α changes from 8 to 16 deg. The tip vortex measured at $x/c > 3$ behaves in a similar way to that at $x/c = 3$ and is not shown. Accordingly, the maximum vorticity, $\omega_{\max}c/U_\infty$, and circulation, $\Gamma/U_\infty c$ (where the tip vortex circulation Γ was estimated by

$$\Gamma = \int_A \omega \, dA$$

where A is an area, over which the magnitude of ω exceeds 2% of that at the vortex center, grow from 21 and 0.2 to 25 and 0.26, respectively. This indicates considerably stronger vortices at $\alpha = 16$ deg than at $\alpha = 8$ deg.

Comparison Between Measured Tip Vortex and Exponential Vortex Solution

Exponential vortex solution is an exact solution to the Navier–Stokes equations (see Ref. 25). The circumferential velocity v_θ is defined by

$$v_\theta = (\Gamma_0/2\pi r)\left[1 - \exp\left(-r^2/r_c^2\right)\right] \tag{1}$$

Because v_r is zero, the vorticity is given by

$$\omega = \frac{\partial v_\theta}{\partial r} - \frac{1}{r}\frac{\partial v_r}{\partial r} + \frac{v_\theta}{r} = \omega_0 \exp\left(-\frac{r^2}{r_c^2}\right) \tag{2}$$

where $\omega_0 = \Gamma_0/\pi r_c^2$.

The circumferential velocity distributions, at $x/c = 3$, normalized by the maximum circumferential velocity $v_{\theta,\max}$ and vortex core radius r_c, and that of the exponential vortex solution are presented in Fig. 4. The measured $v_\theta/v_{\theta,\max}$ at different Reynolds numbers agrees quite well with that of the exponential vortex solution for $r/r_c < 2$ in both $\alpha = 8$ (Fig. 4a) and $\alpha = 16$ deg (Fig. 4b), and a departure is appreciable only for $r/r_c > 2$. Note that the Reynolds number virtually does not affect the measured $v_\theta/v_{\theta,\max}$ within the core of the tip vortex and its effect on $v_\theta/v_{\theta,\max}$ is only discernible outside the core.

Figure 5 shows the $v_\theta/v_{\theta,\max}$ distributions at various downstream stations. At $\alpha = 8$ deg (Fig. 5a), $v_\theta/v_{\theta,\max}$ agrees well with the exponential vortex solution within the vortex core, and good agreement

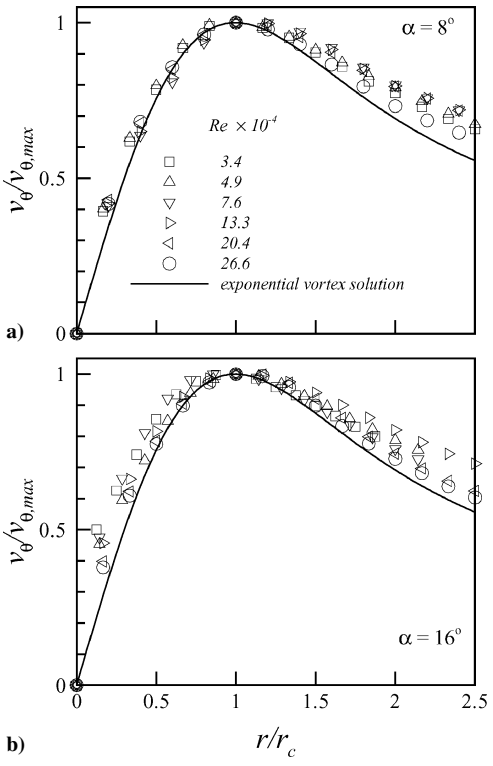

Fig. 4 Averaged circumferential velocity $v_\theta/v_{\theta,\max}$ vs radius r/r_c at different Reynolds numbers, at $x/c = 3$.

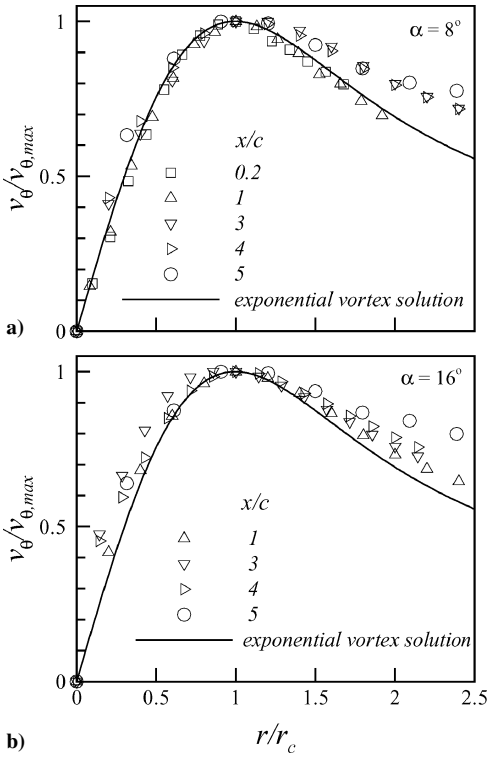

Fig. 5 Averaged circumferential velocity $v_\theta/v_{\theta,\max}$ vs radius r/r_c at different streamwise locations, $Re = 7.6 \times 10^4$.

was found even outside the core at $x/c = 0.2 \sim 1$, where the tip vortex is developing and the viscous effect dominates. Note that the vorticity at the vortex center reaches its maximum at $x/c \approx 1$ for $\alpha = 8$ deg and at $x/c \approx 3$ for $\alpha = 16$ deg. Thus, it is assumed that the vortices are developed beyond these distances. At $x/c = 3$, 4, or 5, the $v_\theta/v_{\theta,\max}$ distributions exhibit a slight deviation at $r/r_c > 1$ from the exponential vortex solution. At $\alpha = 16$ deg (Fig. 5b), the measured $v_\theta/v_{\theta,\max}$ distributions also agree reasonably well with the exponential vortex solution. (The data at $x/c = 0.2$ were not

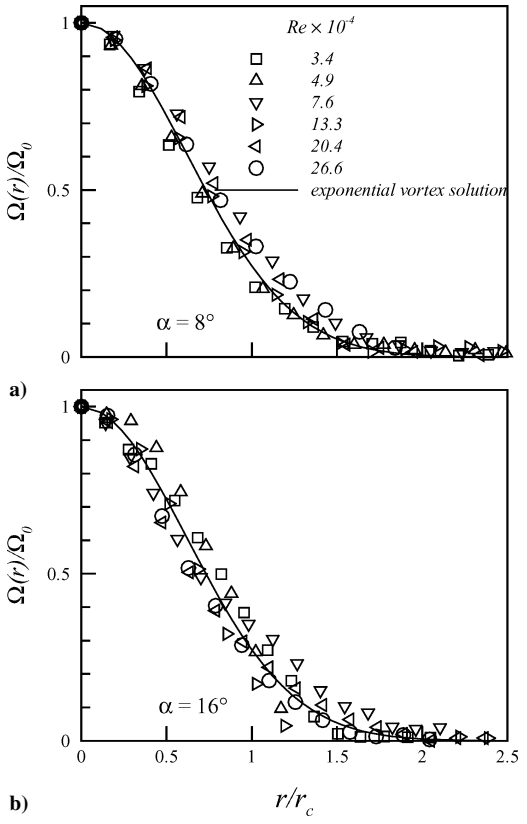

Fig. 6 Vorticity distributions $\Omega(r)$ in radial direction at different Reynolds numbers, $x/c = 3$.

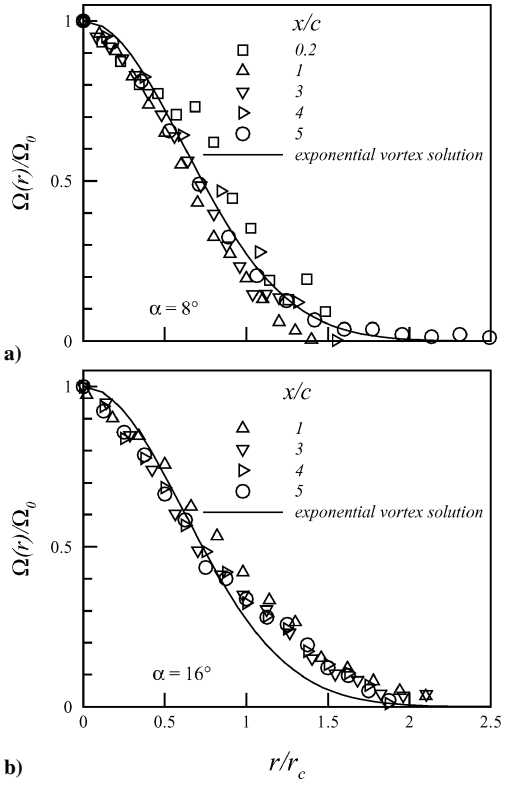

Fig. 7 Vorticity distributions $\Omega(r)$ in radial direction, $Re = 7.6 \times 10^4$.

included; it was difficult to capture the tip vortex at this downstream location.) The deviation becomes significant only at $x/c = 5$. This is probably because the tip vortices grow less coherent at larger x/c.

Vorticity within the tip vortex is not axisymmetrical about the center and varies with θ even at the same radius. To estimate the dependence of ω on r, the mean vorticity at a radius r from the vortex center is defined by

$$\Omega(r) = \frac{1}{2\pi}\int_0^{2\pi} \omega(r,\theta)\,\mathrm{d}\theta, \qquad 0 \le r \le r_m \tag{3}$$

where r_m is the maximum radius at which ω drops to 2% of that at the vortex center.

Figure 6 shows a comparison of $\Omega(r)/\Omega_0$ at $x/c = 3$ for different Reynolds numbers with the exponential vortex solution, where $\Omega_0 \equiv \Omega(0) = \omega(0)$. At all of the Reynolds numbers, the measured $\Omega(r)/\Omega_0$ coincides with that of the exponential vortex solution, regardless of whether the flow around the wing is separated ($\alpha = 16$ deg, Fig. 6b) or not ($\alpha = 8$ deg, Fig. 6a). The measured $\Omega(r)/\Omega_0$ at other x/c values is also in excellent agreement with the exponential vortex solution for $\alpha = 8$ deg (Fig. 7a), but displays a slight deviation at $r/r_c > 1$ for $\alpha = 16$ deg (Fig. 7b).

The circulation Γ_c within the vortex core may be estimated based on ω and r_c. Γ_c/Γ is about 0.66 at $\alpha = 8$ deg for the range of Reynolds number investigated and grows gradually from 0.63 to 0.65 at $\alpha = 16$ deg as Reynolds number increases from 3.4×10^4 to 26.6×10^4. For the exponential vortex solution (laminar), Γ_c/Γ is about 0.72. It is likely that the effect of turbulence leads to the lower measured Γ_c/Γ.

The exponential vortex solution has been used with some success to model vortical structures in the wake, jet, and boundary-layer flows, where the boundary conditions are different from those used to generate the exponential vortex solution. Such a model, though simple and not representative of the real flows, does reproduce the mean velocity and Reynolds stresses reasonably well for these flows. The tip vortices should not agree well with the exponential solution because the vortices are not isolated nor fully developed, and they are not produced by a concentrated line vortex, etc. However, the present results do show agreement between the measured tip vortices and the exponential vortex solution; the deviation outside the core region, as expected, is probably due to turbulent diffusion. This agreement suggests a potential use of the exponential vortex solution for numerical modeling of the wing-tip vortex.

Conclusions

The near-field tip vortices ($x/c \le 5$) generated by a rectangular NACA 0012 half-span wing model have been measured with PIV. The measured tip vortex was compared with the exponential vortex solution. The investigation leads to the following conclusions.

1) The tip vortex formation was intensified as the angle of attack α was increased from 8 deg without leading-edge flow separation to 16 deg with separation. In general, increase in angle of attack led to a larger and stronger tip vortex, as quantified by its increasing maximum streamwise vorticity and circumferential velocity. The circulation $\Gamma/U_\infty c$ of the tip vortex is about 0.2 at $\alpha = 8$ deg and grows to 0.26 at $\alpha = 16$ deg at $Re = 7.6 \times 10^4$.

2) The wing-tip vortex shows little dependence in the circumferential velocity ($v_\theta/v_{\theta,\max}$) and streamwise vorticity [$\Omega(r)/\Omega_0$], when normalized by their local maximum, on the angle of attack, Reynolds number, and downstream distance from the wing. The exponential vortex solution describes reasonably well the wing-tip vortex in terms of the radial distributions of $v_\theta/v_{\theta,\max}$ and $\Omega(r)/\Omega_0$. There is a slight departure outside the core region, probably due to the effect of turbulent diffusions, which cannot be modeled by the exponential vortex solution. Further note that, once the tip vortex is developed, the ratio (Γ_c/Γ) of circulation in the core region to that of the total circulation is 0.63-0.66 (which value is slightly greater for the attached flow at $\alpha = 8$ deg than the separated at $\alpha = 16$ deg), close to that (0.72) of the exponential vortex solution. Again, the turbulence effect probably contributes to the lower Γ_c/Γ in the measured tip vortex than the exponential vortex solution.

Acknowledgment

Y. Zhou wishes to acknowledge support by the Research Grants Council of the Government of the HKSAR through Grant PolyU 5316/03E.

References

[1]Batchelor, G. K., "Axial Flow in Trailing Line Vortices," *Journal of Fluid Mechanics*, Vol. 20, No. 4, 1964, pp. 645–658.

[2]McCormick, B. W., Tangler, J. L., and Sherrieb, H. E., "Structure of Trailing Vortices," *Journal of Aircraft*, Vol. 5, No. 3, 1968, pp. 260–267.

[3]Robins, E. R., and Delisi, D. P., "Potential Hazard of Aircraft Wake Vortices in Ground Effect with Crosswind," *Journal of Aircraft*, Vol. 30, No. 2, 1993, pp. 201–205.

[4]Spalart, P. R., "Airplane Trailing Vortices," *Annual Review of Fluid Mechanics*, Vol. 30, 1998, pp. 107–138.

[5]Rossow, V. J., "Lift-Generated Vortex Wakes of Subsonic Transport Aircraft," *Progress in Aerospace Sciences*, Vol. 35, No. 6, 1999, pp. 507–660.

[6]Liu, Z., Russell, J. W., and Sankar, L. N., "A Study of Rotor Tip Vortex Structure Alteration Techniques," *Journal of Aircraft*, Vol. 38, No. 3, 2001, pp. 473–477.

[7]Devenport, W. J., Rife, M. C., Liapis, S. I., and Follin, G. J., "The Structure and Development of a Wingtip Vortex," *Journal of Fluid Mechanics*, Vol. 312, 1996, pp. 67–106.

[8]Hoijmakers, H. W. M., "Vortex Wakes in Aerodynamics," *Characterisation and Modification of Wakes from Lifting Vehicles in Fluid*, AGARD CP 584, 1996.

[9]Crow, S. C., "Stability Theory for a Pair of Trailing Vortices," *AIAA Journal*, Vol. 8, No. 12, 1970, pp. 2172–2179.

[10]Chow, J. S., Zilliac, G. G., and Bradshaw, P., "Mean and Turbulence Measurements in the Near Field of a Wingtip Vortex," *AIAA Journal*, Vol. 35, No. 10, 1997, pp. 1561–1567.

[11]Shekarriz, A., Fu, T. C., Katz, J., and Huang, T. T., "Near-Field Behavior of a Tip Vortex," *AIAA Journal*, Vol. 31, No. 1, 1993, pp. 112–118.

[12]Dacles-Mariani, J., Zilliac, G. G., Chow, J. S., and Bradshaw, P., "Numerical/Experimental Study of a Wingtip Vortex in the Near Wake," *AIAA Journal*, Vol. 33, No. 9, 1995, pp. 1561–1568.

[13]Francis, T. B., and Katz, J., "Observations on the Development of a Tip Vortex on a Rectangular Hydrofoil," *Journal of Fluids Engineering*, Vol. 110, No. 2, 1988, pp. 208–215.

[14]Smith, D. A. R., "Perturbation of Vortex Wakes for Amelioration of the Vortex Wake Hazard," Ph.D. Dissertation, Dept. of Mechanical Engineering, Imperial College London, London, 2003.

[15]Bearman, P., and Hogan, C., "Experiments on Wake Vortex Control," *Conference on Capacity and Wake Vortices*, Imperial College of Science, London, Sept. 2001.

[16]Huenecke, K., and Huenecke, C., "Flowfield Visualisation in Aircraft Wake Vortex Research," *Proceedings of the 9th International Symposium on Flow Visualisation*, Paper No. 139, Edinburgh, U.K., Aug. 2000.

[17]Yeung, A. F. K., and Lee, B. H. K., "Particle Imaged Velocimetry Study of Wing-Tip Vortices," *AIAA Journal*, Vol. 36, No. 2, 1998, pp. 482–484.

[18]Zhou, Y., and Antonia, R. A., "A Study of Turbulent Vortices in the Near Wake of a Cylinder," *Journal of Fluid Mechanics*, Vol. 453, 1993, pp. 643–661.

[19]Davies, M. E., "A Comparison of the Wake Structure of a Stationary and Oscillating Bluff Body, Using a Conditional Averaging Technique," *Journal of Fluid Mechanics*, Vol. 75, 1976, pp. 209–231.

[20]Oler, J. W., and Goldschmidt, V. W., "A Vortex-Street Model of the Flow in the Similarity Region of a Two-Dimensional Free Turbulent Jet," *Journal of Fluid Mechanics*, Vol. 123, pp. 523–535.

[21]Bisset, D. K., Antonia, R. A., and Browne, L. W. B., "Spatial Organization of Large Structures in the Turbulent Far Wake of a Cylinder," *Journal of Fluid Mechanics*, Vol. 218, 1991, pp. 439–461.

[22]Robinson, S. K., "The Kinematics of Turbulent Boundary Layer Structure," NASA TM 103859, 1991.

[23]Zhou, Y., Zhang, H. J., and Yiu, M. W., "Momentum and Heat Transport in the Turbulent Wake of Two Side-by-Side Cylinders," *Journal of Fluid Mechanics*, Vol. 458, 2002, pp. 303–332.

[24]Huang, R. F., and Lin, C. L., "Vortex Shedding and Shear-Layer Instability of Wind at Low-Reynolds Numbers," *AIAA Journal*, Vol. 33, No. 8, 1995, pp. 1398–1403.

[25]Lamb, H., *Hydrodynamics*, 6th ed., Dover, New York, 1945.